

Supplemental Information to manuscript

Link to online manuscript:

<https://www.frontiersin.org/articles/10.3389/fmars.2019.00295/>

Links between summer phytoplankton community composition and trace metal distribution in the surface waters of the Atlantic Southern Ocean

Johannes J. Viljoen^{1*}, Ian Weir^{1*}, Susanne Fietz^{1,f}, Ryan Cloete¹, Jean Loock¹, Raissa Philibert^{1,2}, Alakendra N. Roychoudhury¹

¹Centre for Trace Metal and Experimental Biogeochemistry, Department of Earth Sciences, University of Stellenbosch, 7600 Stellenbosch, South Africa

²Hatfield Consultants, North Vancouver, British Columbia, Canada

*these authors contributed equally

^fcorresponding author: Department of Earth Sciences, Stellenbosch University, 7600 Stellenbosch, South Africa, sfietz@sun.ac.za, +27218083117

1 Supplementary methods

1.1 Details regarding the choice of specific pigments and phytoplankton groups in the CHEMTAX processing for S54 cruise Good Hope transect.

The interpretation of HPLC pigment data for the assessment of phytoplankton community composition can be difficult due to pigment markers that are present in several groups. However, with the use of the CHEMTAX v1.95 chemical taxonomy software (Mackey et al. 1996), the HPLC-pigment concentration data sets can be used to calculate the contribution of individual phytoplankton functional groups to total chlorophyll-a (chl-a) (used here as a proxy for biomass). The CHEMTAX phytoplankton community composition estimates are based on the relative abundance of a suite of marker pigments to total chl-a, initial ratios, in water of close proximity to the current study area, determined by previous studies (Wright et al. 2010). Essentially the software makes use of the idea that each group has a characteristic set of accessory pigments, but all phytoplankton groups contains chl-a responsible for the contribution to the total chl-a of a community. The CHEMTAX matrix factorisation is therefore based on the ratios between at least two, often various accessory pigments and chl-a per group (Mackey et al. 1996; Wright et al. 2010). These ratios are loaded into the program along with the pigment concentrations determined by HPLC analysis where after it goes through a suite of iterations and provides an estimate of the group contribution to the total chl-a. For the results of the CHEMTAX software to be reliable and as accurate as possible, knowledge on the phytoplankton communities present in the study area is needed in the form of pigment ratios per phytoplankton group (Schlüter et al. 2011). Below we briefly describe the set-up of the CHEMTAX software (choices of groups and their accessory pigments) to process the respective pigment data for the identification of phytoplankton functional groups and determination of their relative abundances for each surface sample taken. We also provide additional explanations on less typical selections of groups and “marker” pigments.

Choice of groups: The main phytoplankton groups to be included into the initial ratio matrix that were used by the CHEMTAX processing were selected based on literature data published for the Atlantic Southern Ocean and nearby regions (Wright et al. 2010; Gibberd et al. 2013; Mendes et al. 2015). Ten phytoplankton groups were chosen: cyanobacteria, prasinophytes, dinoflagellates, cryptophytes, *Phaeocystis*-H (High iron-acclimated state of *Phaeocystis antarctica*), *Phaeocystis*-L (Low iron-acclimated state of *P. antarctica*), cocolithophores (haptophytes-6), pelagophytes (pelago-1), chlorophytes and diatoms. *Phaeocystis*-H and -L here refers exclusively to *P. antarctica* (Wright et al. 2010) but was separated into functional forms acclimated to low and high iron due to the ability of *P. antarctica* to adjust their pigment ratios to various ambient iron concentration and conditions, iron enriched vs. iron depleted conditions (DiTullio et al. 2007). Although it would be the ideal, no separate bins were created according to depth or regional differences as with different zones. This was due to the limitation of samples and HPLC data that only represents surface communities. Therefore, all HPLC pigment data was set to be processed within one run. The optimised ratios after the CHEMTAX analyses can be found in Table S6 and the resulting phytoplankton chl-a concentrations in Table S7. Below we provide further details regarding the choice of specific pigments for the CHEMTAX.

Choice of pigments: The following pigments were included in our analysis: Chl-c3; Chl-c1c2; peridinin (Peri); 19'-butanoyloxyfucoxanthin (19-But); fucoxanthin (Fuco); neoxanthin (Neo); prasinoxanthin (Pras); 19'-hexanoyloxyfucoxanthin (19-Hex); alloxanthin (Allox); zeaxanthin (Zea); Chl-b (Table S5). From the detected pigments, these pigments were selected as two or more of them together are indicative of the identified phytoplankton groups in certain ranges of ratios versus chl-a. Since the published optimised ratios from Wright et al. (2010) for the Southern Ocean do not contain zeaxanthin values and no other literature was found that reports zeaxanthin ratios for phytoplankton studies that include pelagophytes and coccolithophores in the same initial pigment ratio set, ratios for the Indian SAZ from Mendes et al. (2015) were used in our study. Some pigments known to be prominent and suitable marker pigments in other oceanic regions, such as lutein, for example, were below detection limit in our Atlantic Southern Ocean study. In contrast to Viljoen et al. (2018), Allox was detected and was included as it was an indication of the presence of the cryptophyte group. However, to ensure that the number of pigments used for the CHEMTAX analyses is higher than the number of phytoplankton groups (i.e. ten; Mackey et al. 1996), we added the pigment pair chl-c1c2 to the suite of marker pigments used in our CHEMTAX processing. This chl-c1c2 ratio is a combined signal of the chl-c1 and chl-c2 pigments, which could not be separated by the HPLC system used. The chl-c1c2 was included as it was the only pigment left within our HPLC-pigment data set that is not drastically influenced by degradation or photo-acclimation (Supplemental information of Viljoen et al. 2018). The CHEMTAX software does not allow the number of phytoplankton groups to be equal or more than the number of pigments used in the calculations. To adhere to this, diatoms were grouped as total diatoms to reduce the number of phytoplankton and due to the need of both chl-c3 and chl-c1 separate from chl-c2 to distinguish two separate group of diatoms with the use of pigments (Wright et al. 2010).

Pelagophytes (pelago-1), which are not commonly reported in Atlantic Southern Ocean CHEMTAX studies (Gibberd et al. 2013), was included as their presence in our samples was supported by the presence of their dominant marker pigment 19'-butanoyloxyfucoxanthin (19-But; Schlüter et al. 2011). This proved valuable, since the CHEMTAX results showed that they were present in noticeable contributions within a reasonable amount of our samples, especially in the PFZ and AAZ. For all 19-But ratios, the latest and geographically, closest available ratios optimised for the Indian SAZ was used (Mendes et al. 2015).

1.2 Modified colorimetric detection of silicic acid

Concentrations of certain reagents differed slightly from the original method described by Grasshoff (1983). Following the modified method, sulphuric acid (3.6 M) was added to a solution of ammonium molybdate tetrahydrate (20g/100ml) as opposed to sulphuric acid (4.5 M) and ammonium molybdate tetrahydrate (12.7g/100ml) as recommended by Grasshoff (1983). A modified solution of ascorbic acid (1.75g/100ml) was also used, which differed from the 2.8g/100ml recommended by Grasshoff (1983).

1.3 Details on washing procedures in preparation for trace metal sampling

All plastic ware, containers and sample bottles used for the storage of seawater and reagents were extensively acid cleaned according to strict protocols outlined by GEOTRACES (Cutter and Bruland 2012; Cutter et al. 2014). Cleaning consisted of soaking in Extran® (Merck) alkaline detergent for 1 week, 6M HCl (reagent grade, uniLAB®, Merck) for 1 month and 1M HCl (Suprapur®, Merck) for 1 month. Ultra-high purity water (UHPW), produced with the

Milli-Q® Advantage A10 system (Millipore), was used to rinse sample bottles in between cleaning stages (Cloete et al. 2019).

1.4 Details on Trace metal sampling and analysis

Sample collection for the bioactive trace metals Mn, Fe, Co, Ni, Cu, Zn, and Cd followed GEOTRACES guidelines (Cutter et al., 2014; Cutter and Bruland, 2012) inside the on-board class 100 clean container. Seawater samples were collected following a strict clean protocol using a GEOTRACES compliant CTD and rosette. Directly upon recovery of the rosette, the GO-FLO bottles were covered in a polyvinyl chloride (PVC) plastic wrap in addition to their ends being covered in plastic (PVC) shower caps, and were transported into a class 100 clean lab for sub-sampling (Cloete et al. 2019). The collected seawater was filtered for dissolved trace metal determination from the GoFlo bottles into acid-washed 125 mL LDPE bottles through 0.2 µm pore size Acropak™ 500 Supor® membrane filters with filtered (Midisart 2000, 0.20 µm) nitrogen assistance (BIP Technology). All samples were immediately acidified using hydrochloric acid (Ultrapur, Merck) to a pH of 1.7 and stored. A SeaFAST-pico SC-4 DX (Elemental Scientific) module was used for offline pre-concentration (by a factor of 40 times) inside a class 100 trace metal clean laboratory, prior to injection into a quadrupole inductively coupled plasma mass spectrometer (ICP-MS; Agilent 7900) at Stellenbosch University, South Africa. The instrument configuration and chelating resin as well as intercalibration, within laboratory calibration and check standards are provided in (Cloete et al. 2019).

1.5 Comparison to previously reported dissolved trace metal surface values in the Southern Atlantic Ocean

Direct comparisons to previously published trace metal data are best made in the intermediate to deep waters where predictability is significantly higher. Trace metal cycling in the surface can be extremely variable owing to processes such as: bloom depletion, seasonality, changing mixed layer, variable trace metal reservoir sizes, storm-induced mixing, grazing, atmospheric flux, photochemical reduction and sea ice melt. These dynamic surface processes drive persistent change leading to measured surface concentrations typically being accepted as a “snapshot” providing insights into the moment. Nonetheless, the working range of concentrations (Table 1) compares favourably for several elements relative to previously measured concentrations across the transect. Baars et al. (2014) report that Cd concentrations are lowest in the STZ at 5-7 pM increasing to 409-599 pM in the AAZ and Weddell Gyre. Surface Mn was previously quantified between 0.05 nM within the Weddell Gyre (64 °S) up to 0.61 nM within the AAZ (54 °S) according to Middag et al. (2011). Iron was quantified by Klunder et al. (2011) in the range between 0.07 nM (68 °S) and 0.46 nM (69 °S) within the Weddell Gyre with concentrations up to 0.47 nM in the AAZ (54 °S). Croot et al. (2011) report Zn between 0.5 nM in the SAF up to 4.5 nM in the Weddell Gyre. Similarly, Cu was reported by Heller & Croot (2015) between 0.7 nM in the SAF up to 1.8 nM within the Weddell Gyre. Whilst Ni has not been reported on the zero meridian, Loscher (1999) reported concentrations at 40m ranging from 3.5 nM (49 °S) up to 6.75 nM (58 °S) on the 6 °W meridian.

2 Supplemental Tables

Table S1. Frontal positions (latitude and longitude) encountered along the cruise transect (Bonus Good Hope Line) and criteria (temperature and water depth) used for identification of frontal positions following Orsi et al. (1995) and Pollard et al. (2002). Temperature profiles were assessed from the eXpendable BathyThermographs (XBT) transect AX25 (NOAA 2015). Abbreviations: STF - Subtropical Front; SAF - Subantarctic Front; PF - Polar Front; SBdy - Southern Boundary of the Antarctic Circumpolar Current (ACC).

Front	Temp. (°C)	Water Depth (m)	Latitude [N]	Longitude [E]
STF	10	200	-40.4	9.3
SAF	6	200	-44.1	6.4
PF	2	200	-50.4	1.5
SBdy	1.5	350	-55.4	0

Table S2. Averages and ranges of macronutrient concentrations (A) and ratios (B) in the surface seawater of the four distinguished water masses across the Atlantic sector of the Southern Ocean measured during the first (December), third (January) and fourth (February) leg of voyage SANAE54 (see Figure 1 for cruise map). Avg. – average. Nutrient concentration surface profiles are shown in Figure 2, while nutrient ratios along the transect are shown in Supplementary Figure S2.

A)	Zone	H ₄ SiO ₄ (μ M)		NO ₃ ⁻ (μ M)		PO ₄ ²⁻ (μ M)	
		Range	Avg.	Range	Avg.	Range	Avg.
Dec	STZ (34 - 40.4°S)	(0.2-3.8)	1.5	(1.3-7.9)	1.3	(0.00-0.46)	0.2
	SAZ (40.41 - 44°S)	(0.3-10.1)	1.7	(2.7-40.2)	24	(0.36-1.57)	0.9
	PFZ (44.1 - 50.4°S)	(0.3-10.1)	2.1	(20.7-40.2)	30	(0.42-1.57)	1.0
	AAZ (50.4 - 55.4°S)	(4.5-66.8)	24	(10.5-40.1)	30	(0.6-2.9)	1.5
	WG (55.4-70°S)	(37.5-87)	56	(6.8-36.6)	14	(0.57-3.3)	1.7
	STZ (34 - 40.4°S)	N.D.	N.D.	N.D.	N.D.	N.D.	N.D.
Jan	SAZ (40.41 - 44°S)	N.D.	N.D.	N.D.	N.D.	N.D.	N.D.
	PFZ (44.1 - 50.4°S)	(0.7-6.7)	2.7	(5.9-28)	16	(0.03-2.02)	1.1
	AAZ (50.4 - 55.4°S)	(3.6-19.8)	12	(14.3-24)	18	(0.95-1.77)	1.3
	WG (55.4-70°S)	(28.2-84.3)	53	(11.8-25.9)	19	(0.66-2.4)	1.4
	STZ (34 - 40.4°S)	(0-1.7)	0.6	(0.2-0.7)	0.4	(0-0.25)	0.1
	SAZ (40.41 - 44°S)	(0.6-4.3)	0.9	(0.3-8.8)	4.5	(0.06-0.63)	0.4
Feb	PFZ (44.1 - 50.4°S)	(0.6-4.3)	2.2	(4.9-13.4)	9.5	(0.57-1.6)	1.0
	AAZ (50.4 - 55.4°S)	(2.8-98)	24	(12.7-22.1)	17	(0.66-2.4)	1.3
	WG (55.4-70°S)	(18.7-57.1)	41	(6.9-34.4)	13	(0.34-1.86)	1.0

B)	Zone	Si/P (μ mol: μ mol)		Si/N (μ mol: μ mol)		N/P (μ mol: μ mol)	
		Range	Avg.	Range	Avg.	Range	Avg.
Dec	STZ (34 - 40.4°S)	(0-53)	11	(0.03-3.89)	1.8	(0-31.3)	7.8
	SAZ (40.41 - 44°S)	(0.6-3.3)	1.8	(0.03-0.76)	0.2	(94.4-52)	18
	PFZ (44.1 - 50.4°S)	(0.2-8.1)	1.9	(0.01-0.37)	0.1	(16.2-94.9)	35
	AAZ (50.4 - 55.4°S)	(1.7-51)	20	(0.2-4.7)	1.1	(6.3-69)	26
	WG (55.4-70°S)	(21.4-78.5)	37	(2-7.05)	4.2	(3.9-31)	9.5
	STZ (34 - 40.4°S)	N.D.	N.D.	N.D.	N.D.	N.D.	N.D.
Jan	SAZ (40.41 - 44°S)	N.D.	N.D.	N.D.	N.D.	N.D.	N.D.
	PFZ (44.1 - 50.4°S)	(0.5-6.9)	2.5	(0.04-0.44)	0.2	(6.8-32.4)	15
	AAZ (50.4 - 55.4°S)	(3-14.9)	8.7	(0.2-1.01)	0.7	(8-25.4)	14
	WG (55.4-70°S)	(17.7-127)	43	(1.35-6.31)	3.0	(9.5-26)	15
	STZ (34 - 40.4°S)	(0-32.4)	8.8	0.1-4.13	1.8	(0-10)	3.7
	SAZ (40.41 - 44°S)	(0.4-33)	5.0	0.04-3.36	0.8	(1.8-16.3)	11
Feb	PFZ (44.1 - 50.4°S)	(0.9-4.4)	2.2	0.12-0.35	0.2	(5.1-18.9)	9.7
	AAZ (50.4 - 55.4°S)	(2.1-64.3)	19	(0.2-5.03)	1.4	(6.2-23.3)	14
	WG (55.4-70°S)	(20.1-88.3)	45	(1.66-4.06)	3.2	(6.6-38.9)	15

Table S3. Rotated component matrices derived from Principal Component Analysis for (A) trace metal concentrations. B) phytoplankton group chl-a concentrations. Highlighted correlation coefficients indicate significant correlation at 95% confidence interval. The Principal Component Analyses with Varimax rotations were carried out in SPSS.

A)	Component		
	1	2	3
% of variance	40.8	34.9	22.2
Cd	-0.17	0.94	-0.27
Cu	-0.58	0.62	-0.48
Fe	-0.13	-0.03	0.98
Zn	0.95	-0.08	-0.28
Ni	-0.77	0.60	-0.14
Mn	0.98	-0.17	-0.01
Co	-0.14	0.89	0.44

B)	Component			
	1	2	3	4
% of variance	26.1	19.5	18.8	13.0
Cyano.	-0.12	0.96	-0.01	0.04
Prasino.	-0.27	-0.10	0.74	-0.02
Dinoflag.	0.32	-0.06	0.66	-0.21
Crypto.	-0.33	-0.15	-0.03	-0.77
Phaeocy-H	0.84	-0.09	0.44	-0.01
Phaeocy-L	-0.50	-0.17	0.04	0.71
Cocco.	0.74	-0.09	-0.18	0.17
Pelago.	-0.04	-0.04	0.80	0.36
Chloro.	-0.14	0.95	-0.16	-0.01
Diatoms	0.89	-0.21	-0.11	-0.10

Table S4. Metal/P ratio ranking in the surface waters of the six trace metal stations. Sampling longitudes and trace metal concentrations may be found in main text Table 1.

Date	Zone	Lat. (N)	metal/P ratio ranking
5/2/2015	STZ	-36.00	Zn>Ni>Mn>Cu>Fe>Cd>Co
12/1/2015	PFZ	-46.03	Ni>Zn>Cu>Fe>Cd>Mn>Co
14/1/2015	AAZ	-50.71	Ni>Zn>Cu>Cd>Fe>Mn>Co
15/1/2015	AAZ	-54.22	Ni>Zn>Cu>Cd>Fe>Mn>Co
16/1/2015	WG	-60.25	Ni>Cu>Zn>Cd>Fe>Mn>Co
18/1/2015	WG	-65.04	Ni>Cu>Zn>Fe>Cd>Mn>Co
19/1/2015	WG	-67.98	Ni>Zn>Cu>Cd>Mn>Fe>Co

Table S5. Pigment concentrations in $\mu\text{g L}^{-1}$ based on HPLC analysis for the Good Hope transect on this cruise (SANAE54). Resulting CHEMTAX phytoplankton community concentrations are given in table below (Table S7) and displayed in Figure 2 and S2. Additional pigment concentrations and discussed ratios are given in Table S8.

Latitude (N)	Longitude (E)	Date	Month	Chl-c3	Chl-c1c2	Peri	But	Fuco	Neo	Pras	Hex	Allox	Zea	Chl-b	Chl-a
-36.4249	13.166	12/6/2014	Dec	0.0000	0.0000	0.0000	0.0000	0.0000	0.0000	0.0051	0.0000	0.0144	0.0000	0.0303	
-39.0427	11.4504	12/7/2014	Dec	0.0000	0.0115	0.0058	0.0060	0.0126	0.0000	0.0000	0.0286	0.0000	0.0039	0.0075	0.0962
-41.7949	8.6075	2/14/2015	Feb	0.0000	0.0046	0.0000	0.0044	0.0096	0.0000	0.0000	0.0218	0.0000	0.0000	0.0000	0.0480
-44.4375	7.1044	12/9/2014	Dec	0.0046	0.0095	0.0000	0.0068	0.0183	0.0000	0.0000	0.0175	0.0000	0.0024	0.0000	0.0742
-44.6305	6.2283	2/13/2015	Feb	0.0050	0.0083	0.0041	0.0060	0.0130	0.0000	0.0021	0.0309	0.0000	0.0000	0.0000	0.0840
-46.0015	7.3337	1/12/2015	Jan	0.0089	0.0225	0.0093	0.0121	0.0816	0.0000	0.0000	0.0803	0.0000	0.0000	0.0000	0.1828
-49.1514	2.4357	12/10/2014	Dec	0.0196	0.0299	0.0114	0.0365	0.0335	0.0000	0.0000	0.0436	0.0000	0.0032	0.0109	0.1826
-49.1984	2.137	2/12/2015	Feb	0.0066	0.0146	0.0000	0.0027	0.0307	0.0000	0.0000	0.0208	0.0000	0.0000	0.0000	0.1000
-50.1477	2.429	1/14/2015	Jan	0.0000	0.0041	0.0000	0.0081	0.0177	0.0000	0.0028	0.0225	0.0000	0.0000	0.0052	0.0725
-52.1328	-0.002	12/11/2014	Dec	0.0079	0.0166	0.0000	0.0072	0.0443	0.0000	0.0000	0.0184	0.0000	0.0000	0.0071	0.1190
-52.8469	1.541	2/11/2015	Feb	0.0000	0.0122	0.0053	0.0000	0.0290	0.0000	0.0000	0.0075	0.0031	0.0000	0.0000	0.0971
-53.5562	2.429	1/14/2015	Jan	0.0204	0.0452	0.0518	0.0134	0.1492	0.0000	0.0000	0.0293	0.0000	0.0000	0.0083	0.2861
-54.6081	2.828	12/12/2014	Dec	0.0065	0.0151	0.0085	0.0046	0.0338	0.0000	0.0000	0.0130	0.0011	0.0000	0.0000	0.1002
-57.5542	-1.7895	1/1/2015	Jan	0.0087	0.0325	0.0000	0.0014	0.1018	0.0000	0.0000	0.0121	0.0000	0.0033	0.0000	0.2079
-58.3048	-0.0017	12/13/2014	Dec	0.0148	0.0404	0.0080	0.0083	0.1025	0.0000	0.0000	0.0265	0.0000	0.0000	0.0000	0.2253
-59.722	-0.0027	1/16/2015	Jan	0.0091	0.0188	0.0000	0.0067	0.0698	0.0000	0.0000	0.0272	0.0000	0.0000	0.0000	0.1421
-62.1655	-3.069	12/31/2014	Dec	0.0097	0.0289	0.0000	0.0026	0.0579	0.0000	0.0000	0.0543	0.0000	0.0039	0.0082	0.1929
-62.823	-0.4718	12/14/2014	Dec	0.0160	0.0456	0.0043	0.0056	0.1087	0.0000	0.0000	0.0300	0.0000	0.0000	0.0000	0.2339
-65.0015	0.6542	1/18/2015	Jan	0.0263	0.0650	0.0077	0.0054	0.1479	0.0000	0.0000	0.0582	0.0000	0.0000	0.0000	0.2765
-66.6125	-1.4187	12/15/2014	Dec	0.0000	0.0029	0.0000	0.0016	0.0150	0.0000	0.0000	0.0045	0.0000	0.0000	0.0000	0.0437
-67.638	-0.0045	1/19/2015	Jan	0.0567	0.1397	0.0075	0.0133	0.2211	0.0000	0.0000	0.2652	0.0000	0.0000	0.0000	0.5704
-69.792	-1.9392	1/20/2015	Jan	0.0192	0.0705	0.0039	0.0055	0.1833	0.0000	0.0000	0.0418	0.0000	0.0000	0.0000	0.3773
-70.034	-2.6444	12/16/2014	Dec	0.0080	0.0254	0.0000	0.0045	0.0965	0.0000	0.0000	0.0851	0.0000	0.0000	0.0000	0.2597
-70.09	-1.5887	1/23/2015	Jan	0.0035	0.0129	0.0000	0.0027	0.0410	0.0000	0.0024	0.0085	0.0015	0.0000	0.0128	0.1140

Table S6. Pigment:Chl-a ratios used in CHEMTAX analysis of pigment data: (a) initial ratios before analysis and b) final optimised ratios after analysis. Abbreviations: Chl, chlorophyll; Peri, peridinin; 19-But, 19'-butanoyloxyfucoxanthin; Fuco, fucoxanthin; Neo, neoxanthin; Pras, prasinoxanthin; 19-Hex, 19'-hexanoyloxyfucoxanthin; Allox, alloxanthin; Zea, zeaxanthin. Data sources for (a): Chl-c1c2, Diatoms and Coccolithophores (Haptophytes-6; Gibberd et al., 2013: G3 and G4), 19-But, Zea and Pelagophytes (Mendes et al., 2015: SAZ), all other values (Wright et al. 2010).

a) Initial Pigment Ratios											
Class / Pigment	Chl-c3	Chl-c1c2	Peri	19-But	Fuco	Neo	Pras	19-Hex	Allox	Zea	Chl-b
<i>Cyanobacteria</i>	0	0	0	0	0	0	0	0	0	1.742	0
<i>Prasinophytes</i>	0	0	0	0	0	0.07	0.09	0	0	0.042	0.55
<i>Dinoflagellates</i>	0	0.217	0.82	0	0	0	0	0	0	0	0
<i>Cryptophytes</i>	0	0.127	0	0	0	0	0	0	0.21	0	0
<i>Phaeocystis-H</i>	0.34	0.137	0	0.153	0.13	0	0	0.43	0	0	0
<i>Phaeocystis-L</i>	0.13	0.184	0	0.153	0.01	0	0	1.21	0	0	0
<i>Coccolithophores</i>	0.133	0.135	0	0.006	0.142	0	0	1.092	0	0	0
<i>Pelagophytes</i>	0.175	0.607	0	1.511	0.213	0	0	0	0	0	0
<i>Chlorophytes</i>	0	0	0	0	0	0.071	0	0	0	0.594	0.15
<i>Diatoms</i>	0.067	0.214	0	0	1.078	0	0	0	0	0	0
b) Final Optimized Pigment Ratios											
Class / Pigment	Chl-c3	Chl-c1c2	Peri	19-But	Fuco	Neo	Pras	19-Hex	Allox	Zea	Chl-b
<i>Cyanobacteria</i>	0	0	0	0	0	0	0	0	0	0.635	0
<i>Prasinophytes</i>	0	0	0	0	0	0.031	0.052	0	0	0.024	0.317
<i>Dinoflagellates</i>	0	0.107	0.403	0	0	0	0	0	0	0	0
<i>Cryptophytes</i>	0	0.095	0	0	0	0	0	0	0.157	0	0
<i>Phaeocystis-H</i>	0.155	0.063	0	0.070	0.059	0	0	0.196	0	0	0
<i>Phaeocystis-L</i>	0.016	0.054	0	0.047	0.003	0	0	0.375	0	0	0
<i>Coccolithophores</i>	0.053	0.054	0	0.002	0.057	0	0	0.435	0	0	0
<i>Pelagophytes</i>	0.050	0.173	0	0.431	0.061	0	0	0	0	0	0
<i>Chlorophytes</i>	0	0	0	0	0	0.039	0	0	0	0.327	0.083
<i>Diatoms</i>	0.009	0.083	0	0	0.315	0	0	0	0	0	0

Table S7. Contribution of CHEMTAX phytoplankton groups to Chl-a. Values represent the concentration of each phytoplankton group ($\mu\text{g L}^{-1}$ chl-a), per sample.

Latitude (N)	Longitude (E)	Date	Month	Chl-a	Cyanobacteria	Prasinophytes	Dinoflagellates	Cryptophytes	Phaeocystis-H	Phaeocystis-L	Coccolithophores	Pelagophytes	Chlorophytes	Diatoms
-36.4249	13.166	12/6/2014	Dec	0.0303	0.0108	0.0000	0.0000	0.0005	0.0000	0.0036	0.0037	0.0000	0.0008	0.0109
-39.0427	11.4504	12/7/2014	Dec	0.0962	0.0020	0.0140	0.0076	0.0004	0.0000	0.0411	0.0000	0.0016	0.0000	0.0295
-41.7949	8.6075	2/14/2015	Feb	0.0480	0.0000	0.0000	0.0000	0.0001	0.0000	0.0304	0.0000	0.0011	0.0000	0.0164
-44.4375	7.1044	12/9/2014	Dec	0.0742	0.0014	0.0000	0.0000	0.0002	0.0094	0.0206	0.0000	0.0026	0.0003	0.0397
-44.6305	6.2283	2/13/2015	Feb	0.0840	0.0000	0.0007	0.0053	0.0002	0.0103	0.0390	0.0000	0.0007	0.0000	0.0278
-46.0015	7.3337	1/12/2015	Jan	0.1828	0.0000	0.0000	0.0102	0.0000	0.0000	0.0386	0.0386	0.0047	0.0000	0.0907
-49.1514	2.4357	12/10/2014	Dec	0.1826	0.0014	0.0197	0.0143	0.0001	0.0442	0.0351	0.0000	0.0181	0.0000	0.0496
-49.1984	2.137	2/12/2015	Feb	0.1000	0.0000	0.0000	0.0000	0.0005	0.0129	0.0099	0.0089	0.0000	0.0000	0.0677
-50.1477	2.429	1/14/2015	Jan	0.0725	0.0000	0.0104	0.0000	0.0000	0.0000	0.0316	0.0000	0.0035	0.0000	0.0270
-52.1328	-0.002	12/11/2014	Dec	0.1190	0.0000	0.0126	0.0000	0.0000	0.0137	0.0003	0.0115	0.0034	0.0000	0.0775
-52.8469	1.541	2/11/2015	Feb	0.0971	0.0000	0.0001	0.0069	0.0162	0.0000	0.0055	0.0021	0.0000	0.0001	0.0662
-53.5562	2.429	1/14/2015	Jan	0.2861	0.0000	0.0125	0.0556	0.0000	0.0400	0.0000	0.0047	0.0037	0.0000	0.1696
-54.6081	2.828	12/12/2014	Dec	0.1002	0.0000	0.0000	0.0104	0.0053	0.0148	0.0083	0.0004	0.0010	0.0000	0.0599
-57.5542	-1.7895	1/1/2015	Jan	0.2079	0.0019	0.0000	0.0000	0.0001	0.0121	0.0000	0.0068	0.0000	0.0000	0.1871
-58.3048	-0.0017	12/13/2014	Dec	0.2253	0.0000	0.0000	0.0095	0.0000	0.0274	0.0000	0.0122	0.0025	0.0000	0.1736
-59.722	-0.0027	1/16/2015	Jan	0.1421	0.0000	0.0000	0.0000	0.0000	0.0119	0.0000	0.0192	0.0030	0.0000	0.1080
-62.1655	-3.069	12/31/2014	Dec	0.1929	0.0019	0.0147	0.0001	0.0006	0.0074	0.0150	0.0383	0.0000	0.0000	0.1148
-62.823	-0.4718	12/14/2014	Dec	0.2339	0.0000	0.0000	0.0050	0.0001	0.0299	0.0000	0.0139	0.0005	0.0000	0.1844
-65.0015	0.6542	1/18/2015	Jan	0.2765	0.0000	0.0000	0.0082	0.0000	0.0397	0.0000	0.0305	0.0000	0.0000	0.1981
-66.6125	-1.4187	12/15/2014	Dec	0.0437	0.0000	0.0001	0.0000	0.0002	0.0000	0.0078	0.0000	0.0007	0.0001	0.0349
-67.638	-0.0045	1/19/2015	Jan	0.5704	0.0000	0.0000	0.0085	0.0003	0.0566	0.0000	0.1956	0.0019	0.0000	0.3076
-69.792	-1.9392	1/20/2015	Jan	0.3773	0.0000	0.0000	0.0046	0.0002	0.0283	0.0000	0.0249	0.0007	0.0000	0.3186
-70.034	-2.6444	12/16/2014	Dec	0.2597	0.0000	0.0001	0.0000	0.0000	0.0000	0.0514	0.0423	0.0000	0.0001	0.1658
-70.09	-1.5887	1/23/2015	Jan	0.1140	0.0000	0.0231	0.0000	0.0071	0.0038	0.0000	0.0062	0.0014	0.0000	0.0724

Table S8. Additional pigment concentrations in $\mu\text{g L}^{-1}$ not used in the group estimations, for specific pigment groupings and ratios sample. Phaeo = Phaeophorbide-a (Phorb) + Phaeophytin-a (Phyt), DDT = DD (Diadinoxanthin) + DT (Diatoxanthin), FH = Fucoxanthin (Fuco) + 19'-hexanoyloxyfucoxanthin (Hex).

Latitude (N)	Longitude (E)	Date	Month	Chl-a	Phorb	Diadino	Diato	Phyt	Phaeo	DDT	Fuco+Hex	DDT:FH	DDT:Chla	Phaeo:Chla
-36.4249	13.166	12/6/2014	Dec	0.0303	0.0000	0.0000	0.0000	0.0000	0.0000	0.0051	0.0000	0.0000	0.0000	
-39.0427	11.4504	12/7/2014	Dec	0.0962	0.0000	0.0048	0.0000	0.0000	0.0000	0.0048	0.0412	0.1165	0.0499	0.0000
-41.7949	8.6075	2/14/2015	Feb	0.0480	0.0000	0.0021	0.0000	0.0000	0.0000	0.0021	0.0314	0.0669	0.0438	0.0000
-44.4375	7.1044	12/9/2014	Dec	0.0742	0.0000	0.0040	0.0016	0.0000	0.0000	0.0056	0.0358	0.1564	0.0755	0.0000
-44.6305	6.2283	2/13/2015	Feb	0.0840	0.0000	0.0042	0.0000	0.0000	0.0000	0.0042	0.0439	0.0957	0.0500	0.0000
-46.0015	7.3337	1/12/2015	Jan	0.1828	0.0000	0.0144	0.0000	0.0000	0.0000	0.0144	0.1619	0.0889	0.0788	0.0000
-49.1514	2.4357	12/10/2014	Dec	0.1826	0.0000	0.0097	0.0038	0.0000	0.0000	0.0135	0.0771	0.1751	0.0739	0.0000
-49.1984	2.137	2/12/2015	Feb	0.1000	0.0000	0.0050	0.0000	0.0000	0.0000	0.0050	0.0515	0.0971	0.0500	0.0000
-50.1477	2.429	1/14/2015	Jan	0.0725	0.0000	0.0039	0.0000	0.0000	0.0000	0.0039	0.0402	0.0970	0.0538	0.0000
-52.1328	-0.002	12/11/2014	Dec	0.1190	0.0000	0.0061	0.0000	0.0000	0.0000	0.0061	0.0627	0.0973	0.0513	0.0000
-52.8469	1.541	2/11/2015	Feb	0.0971	0.0000	0.0037	0.0000	0.0000	0.0000	0.0037	0.0365	0.1014	0.0381	0.0000
-53.5562	2.429	1/14/2015	Jan	0.2861	0.0144	0.0179	0.0000	0.0051	0.0195	0.0179	0.1785	0.1003	0.0626	0.0682
-54.6081	2.828	12/12/2014	Dec	0.1002	0.0000	0.0036	0.0015	0.0000	0.0000	0.0051	0.0468	0.1090	0.0509	0.0000
-57.5542	-1.7895	1/1/2015	Jan	0.2079	0.0301	0.0147	0.0089	0.0000	0.0301	0.0236	0.1139	0.2072	0.1135	0.1448
-58.3048	-0.0017	12/13/2014	Dec	0.2253	0.0129	0.0092	0.0046	0.0000	0.0129	0.0138	0.1290	0.1070	0.0613	0.0573
-59.722	-0.0027	1/16/2015	Jan	0.1421	0.0000	0.0098	0.0000	0.0000	0.0000	0.0098	0.0970	0.1010	0.0690	0.0000
-62.1655	-3.069	12/31/2014	Dec	0.1929	0.0000	0.0100	0.0043	0.0000	0.0000	0.0143	0.1122	0.1275	0.0741	0.0000
-62.823	-0.4718	12/14/2014	Dec	0.2339	0.0229	0.0166	0.0033	0.0000	0.0229	0.0199	0.1387	0.1435	0.0851	0.0979
-65.0015	0.6542	1/18/2015	Jan	0.2765	0.0500	0.0202	0.0031	0.0042	0.0542	0.0233	0.2061	0.1131	0.0843	0.1960
-66.6125	-1.4187	12/15/2014	Dec	0.0437	0.0000	0.0035	0.0000	0.0000	0.0000	0.0035	0.0195	0.1795	0.0801	0.0000
-67.638	-0.0045	1/19/2015	Jan	0.5704	0.0157	0.0445	0.0000	0.0000	0.0157	0.0445	0.4863	0.0915	0.0780	0.0275
-69.792	-1.9392	1/20/2015	Jan	0.3773	0.0130	0.0196	0.0000	0.0080	0.0210	0.0196	0.2251	0.0871	0.0519	0.0557
-70.034	-2.6444	12/16/2014	Dec	0.2597	0.0000	0.0148	0.0029	0.0000	0.0000	0.0177	0.1816	0.0975	0.0682	0.0000
-70.09	-1.5887	1/23/2015	Jan	0.1140	0.0062	0.0034	0.0000	0.0000	0.0062	0.0034	0.0495	0.0687	0.0298	0.0544

3 Supplemental Figures

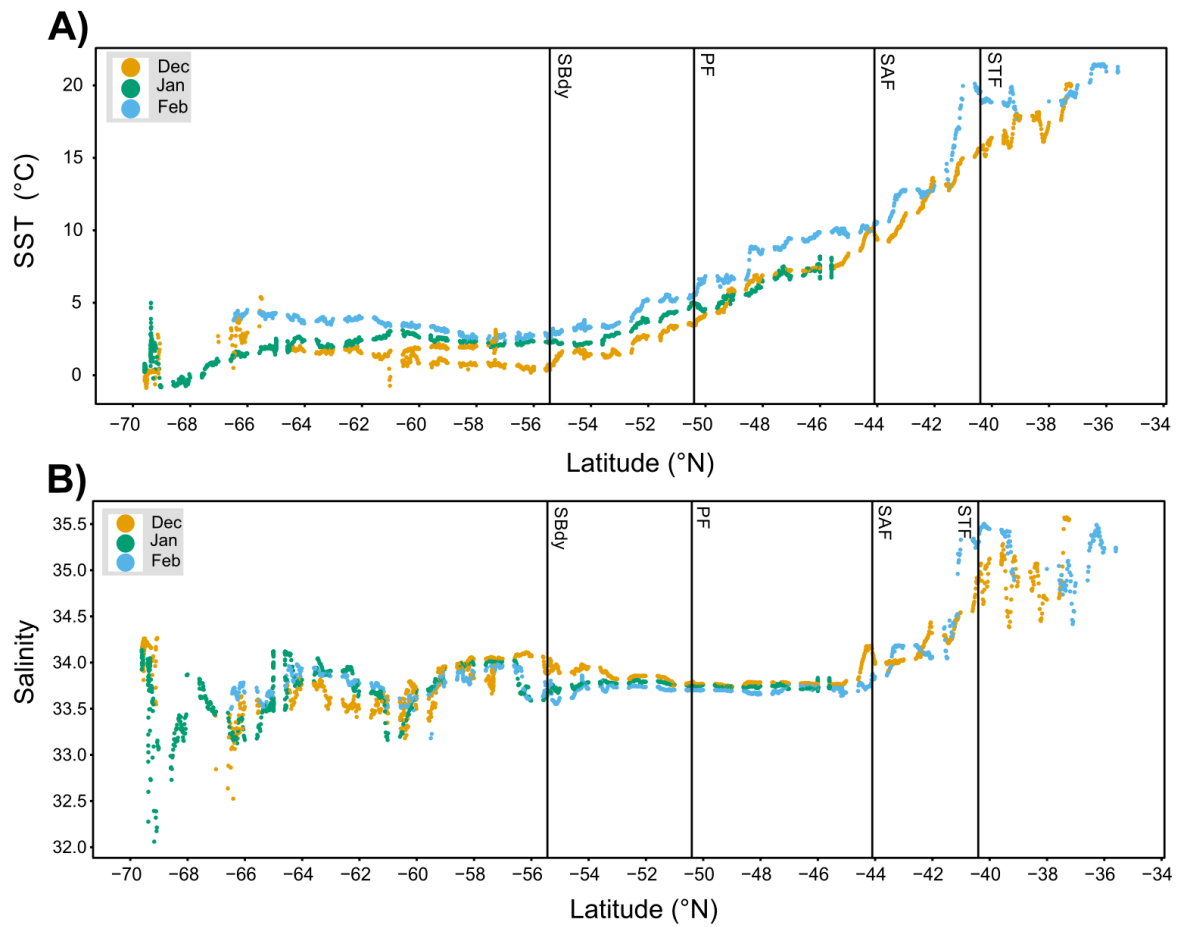


Figure S1. Sea Surface (ca. 5-6m) Temperature (a; SST) and salinity (b) along the Good Hope Line during the first (05/12/2014 – 16/12/2014; “December”), third (29/12/2014 – 6/1/2015; “January”) and fourth (7/2/2015 – 15/2/2015; “February”) legs of voyage SANAЕ54 on board R/V SA Agulhas II.

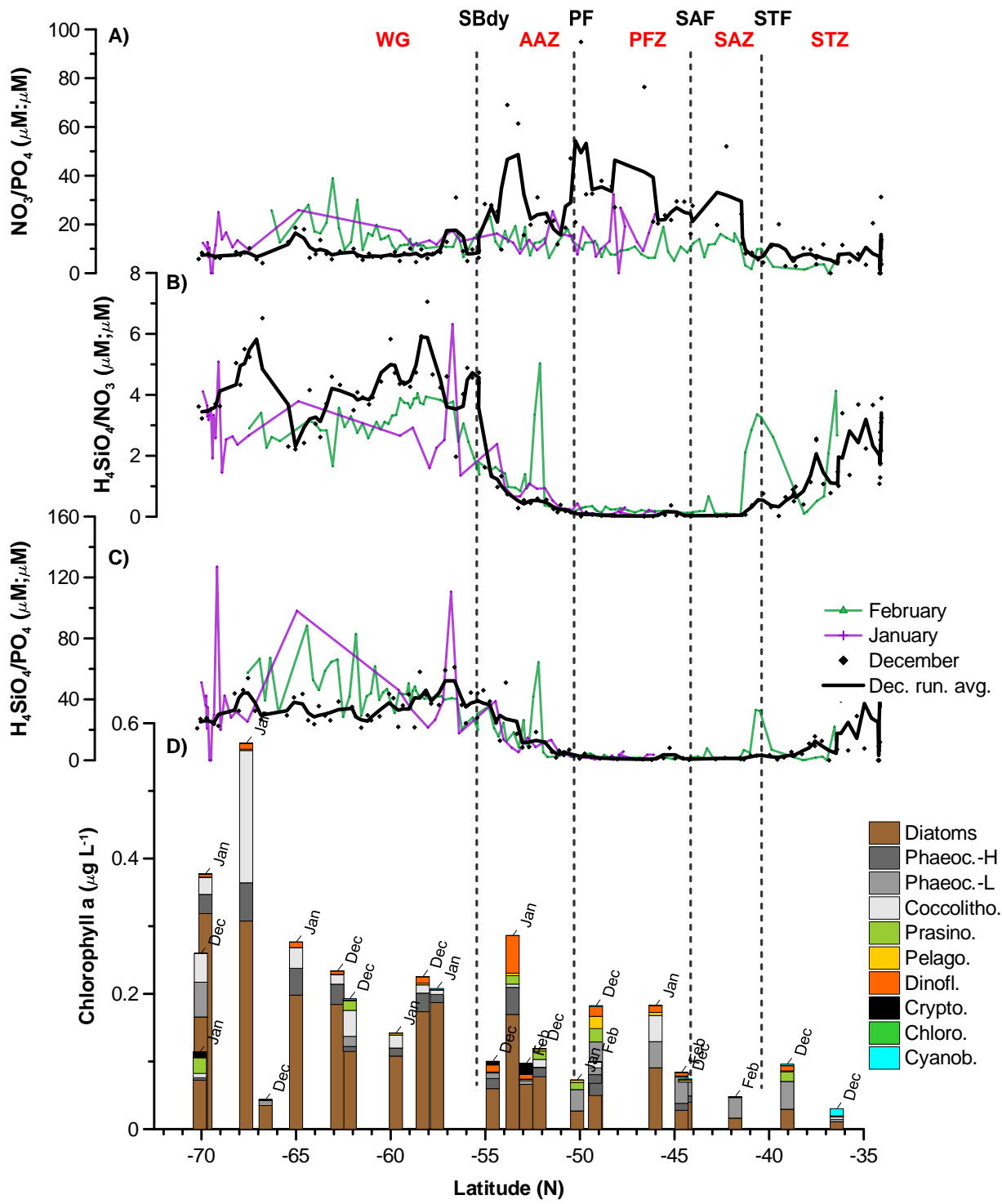


Figure S2. Surface seawater macronutrient ratios A) N/P, B) Si:N and C) Si:P and D) phytoplankton community composition along the transect. Detailed phytoplankton concentrations and contributions to chl-a can be found in Table S5 and S7.

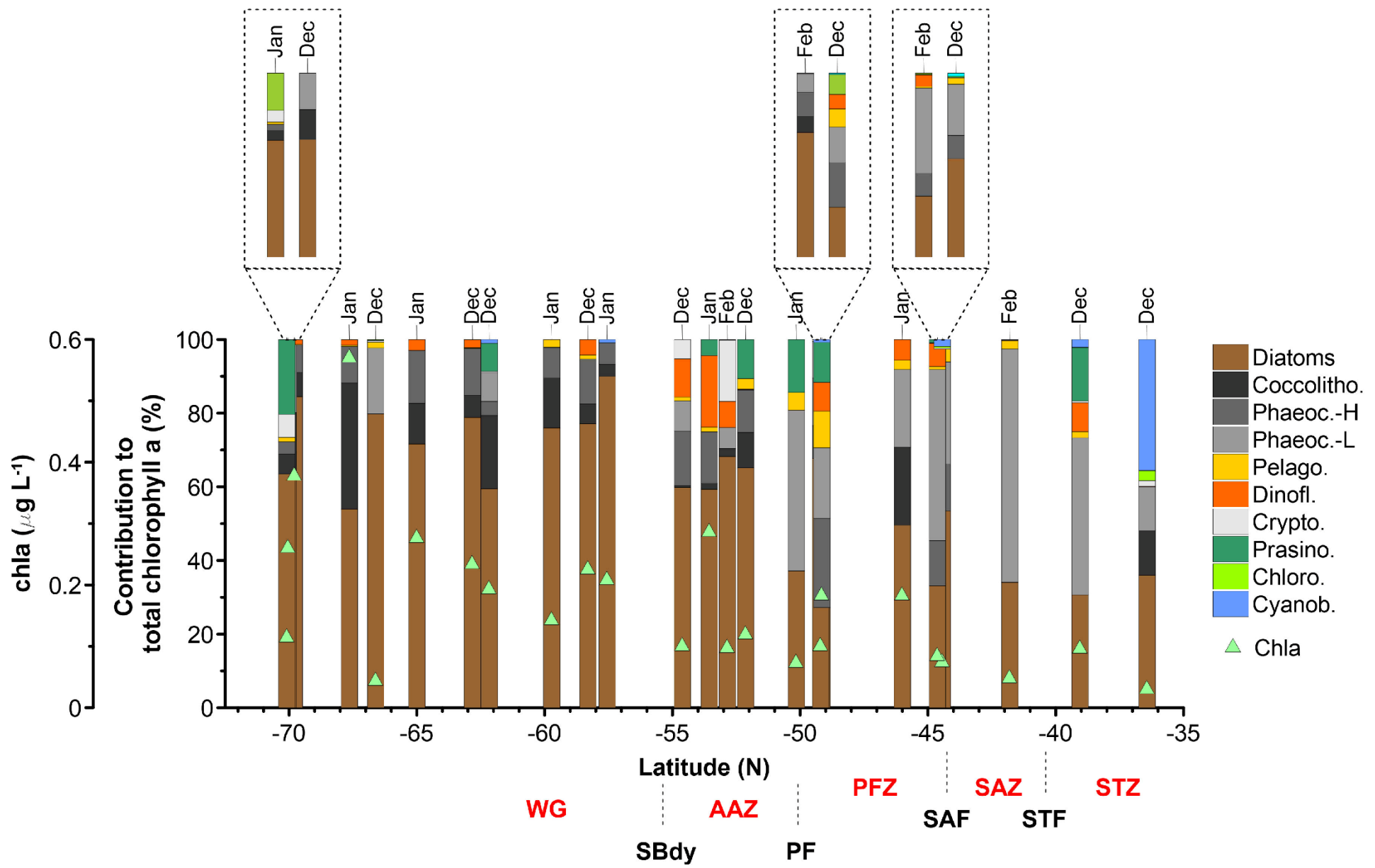


Figure S3 (Previous page). Surface seawater phytoplankton group percentage compositions to total chla (100%) and concentration of total chla (triangle symbol). Some stations were re-visited between December and February. For example, the station at 49 °S was revisited in February, revealing a shift to a diatom-dominated community. February N/P molar ratios (~14:1) agree with a shift to more diatom-dominated waters (Smith and Asper 2001). An increase in SST from December to February (5.8 to 6.5 °C) may potentially have increased water column stability, resulting in a more stratified water column and shallower mixed layer favouring diatom growth (Arrigo 1999). Silicic acid concentrations increased slightly, and phosphate concentrations remained similar from December to February. Conversely nitrate was largely removed to near-limiting concentrations, suggestive of a late summer community removing nitrate at a much more rapid rate than other macronutrients. Low chl-a concentrations, coupled with rapid, preferential, nitrate removal suggest that there might be another factor, such as heterotrophic bacterial uptake (Kirchman and Wheeler 1998) responsible for the large nitrate removal with seasonal progression.

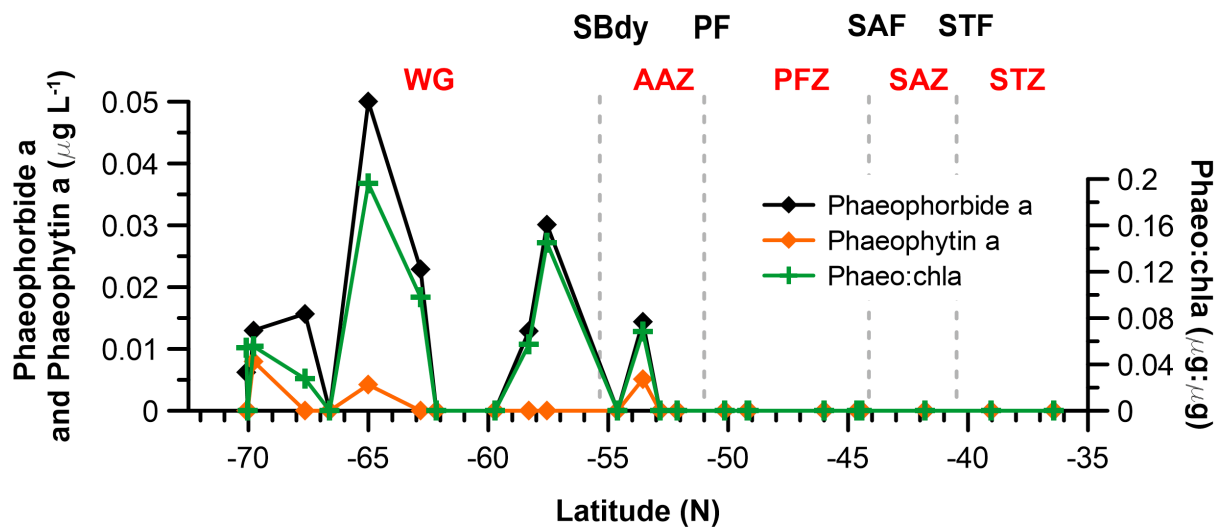


Figure S4. Transect profiles of pigments indicative of degradation: Phaeopigments (Phaeophorbide-a and Phaeophytin-a) concentrations, and ratio of phaeopigment (sum of phaeophorbide plus phaeophytin) versus chl-a (Phaeo:chl-a). Detailed concentrations and ratios can be found in Table S8.

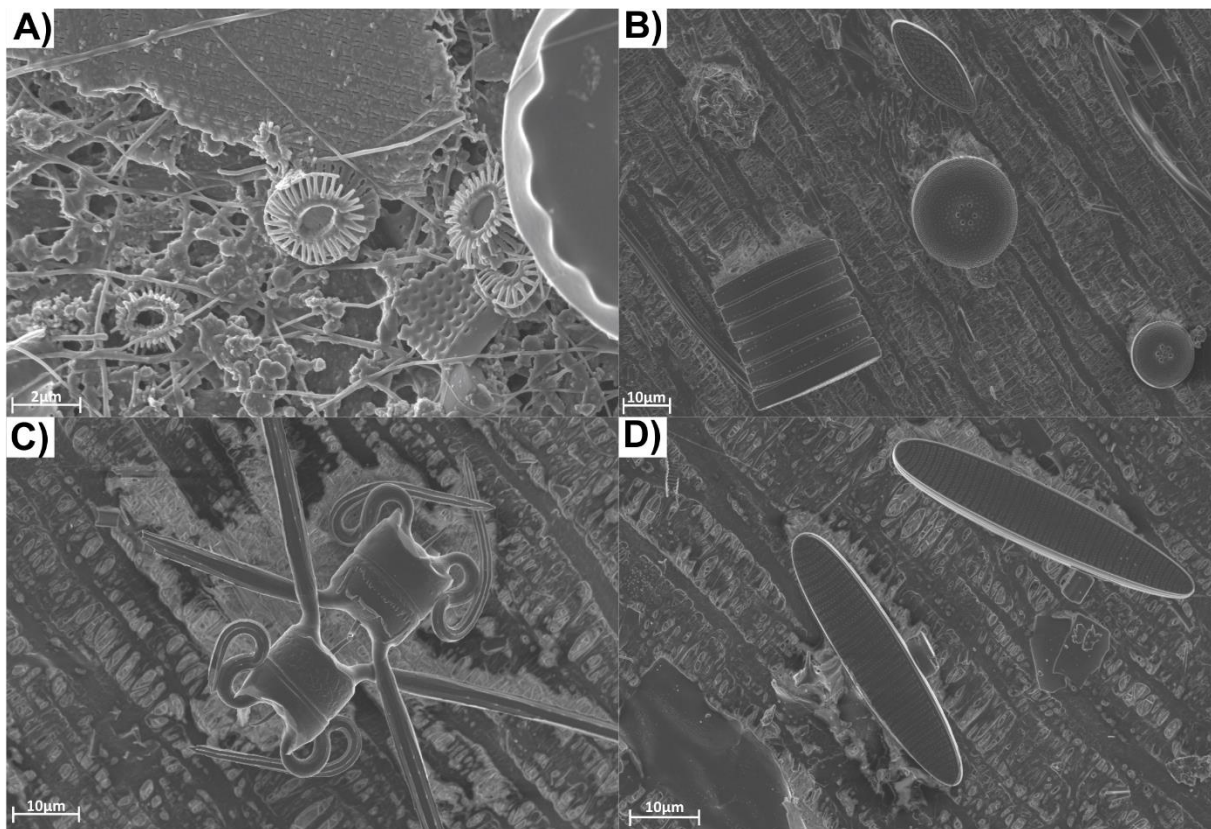


Figure S5 SEM images of dominant diatom species at station 56°S and A) Coccolith platelets B) *Fragilaropsis kerguelensis* both chain-forming and solitary cells (*Fragilaropsis* spp.), *Thalassiosira* spp. C) *Chaetoceros* spp. D) *Fragiliaria* spp.

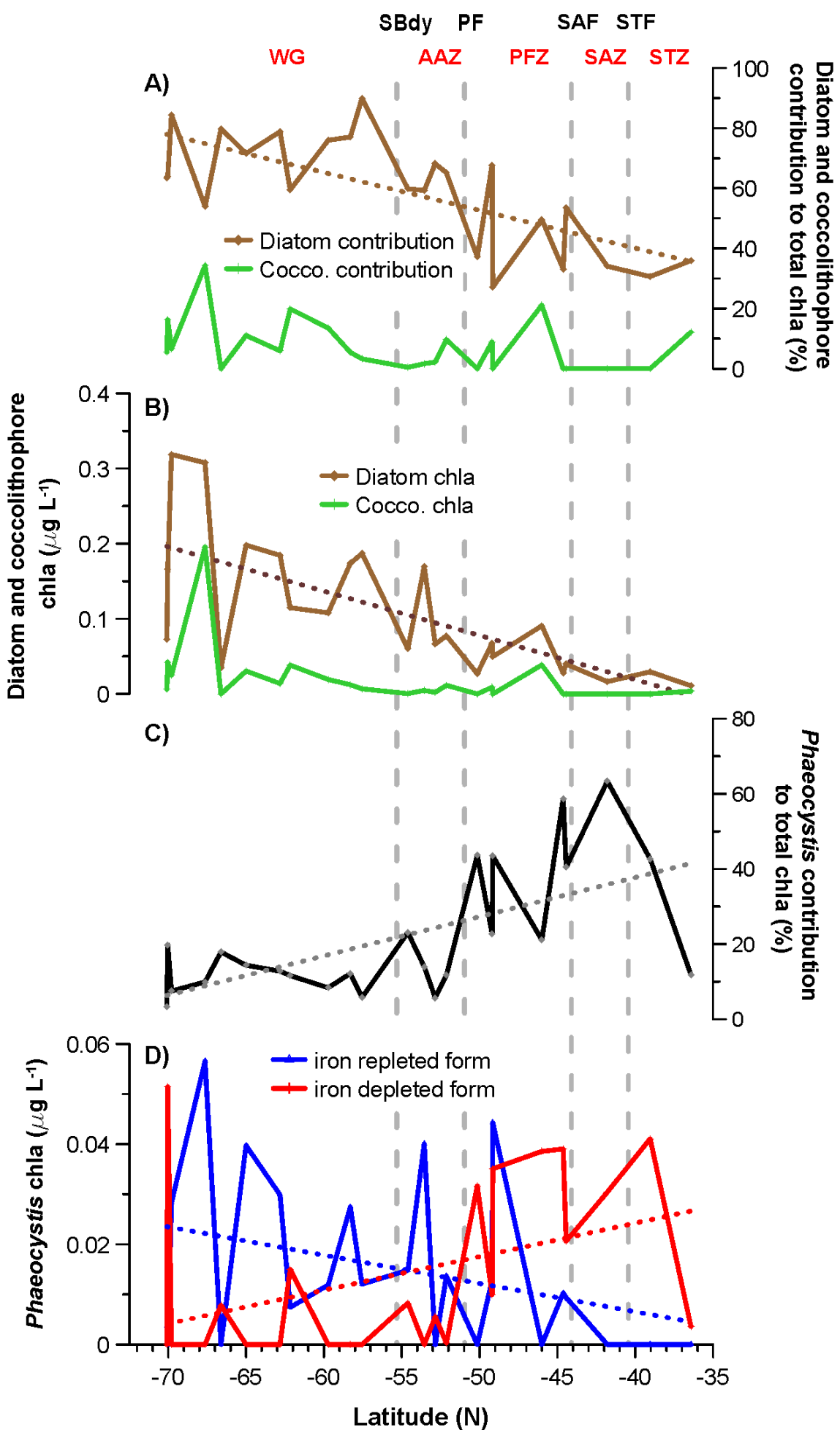
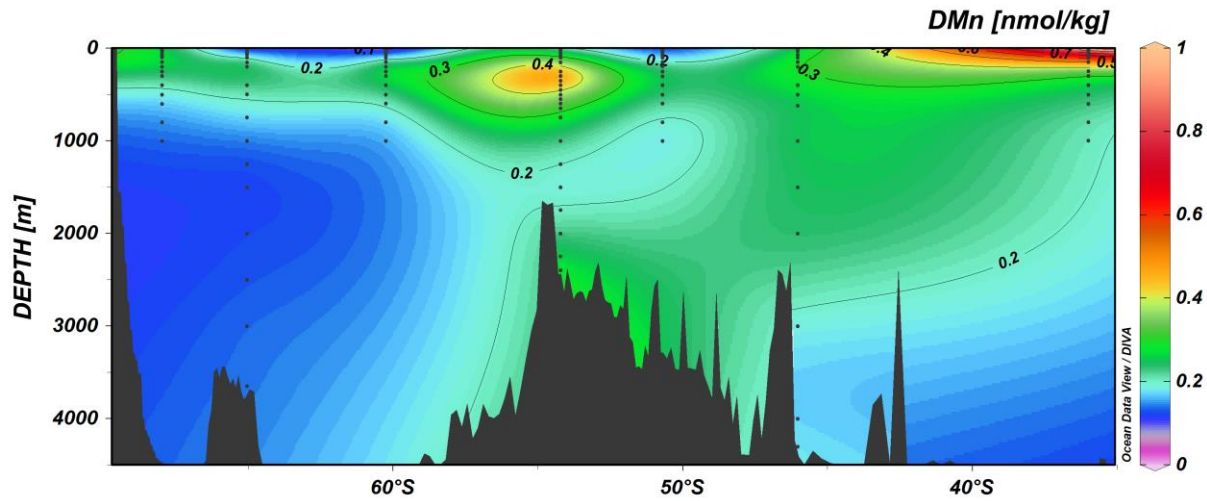


Figure S6. (Previous page). Trends in diatom (A, B) and *Phaeocystis antarctica* (C,D) distribution along Good Hope Line transect. The trends in contribution and in group-specific chl-a are estimated based on the marker pigments composition using CHEMTAX matrix factorisation software (Mackey et al. 1996; Wright et al. 2010). (A) diatom contribution to total chl-a, B) chl-a derived from diatoms, C) *Phaeocystis* contribution to total chl-a, D) chl-a derived from *Phaeocystis*, which can be distinguished into forms acclimated to high iron concentrations and forms acclimated to low iron concentrations (Wright et al. 2010). The coefficient of determination for diatom contribution (%) is $R^2 = 0.49$. Detailed phytoplankton concentrations and contributions to chl- can be found in Table S5 and S7.

A)



B)

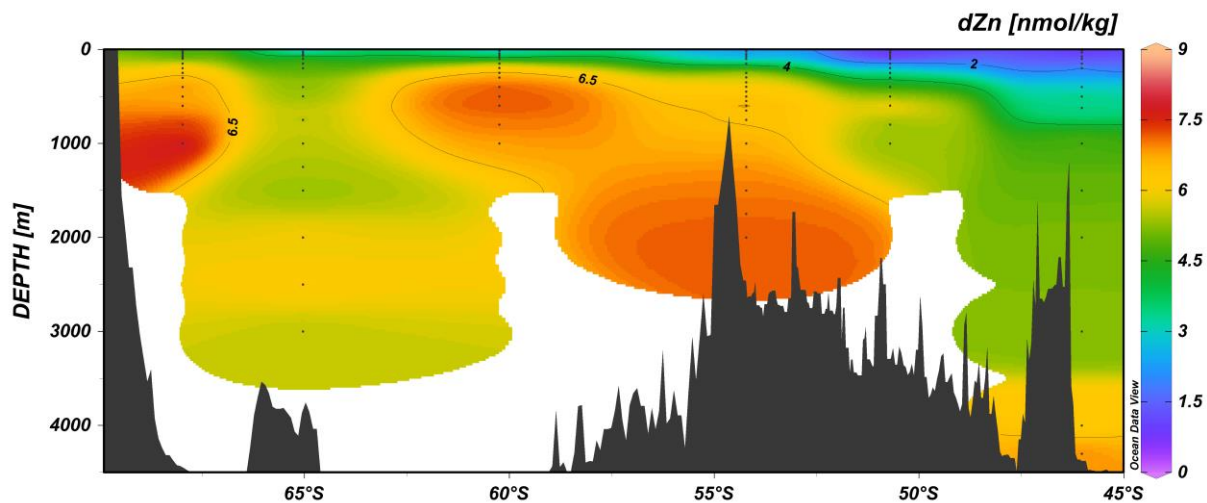
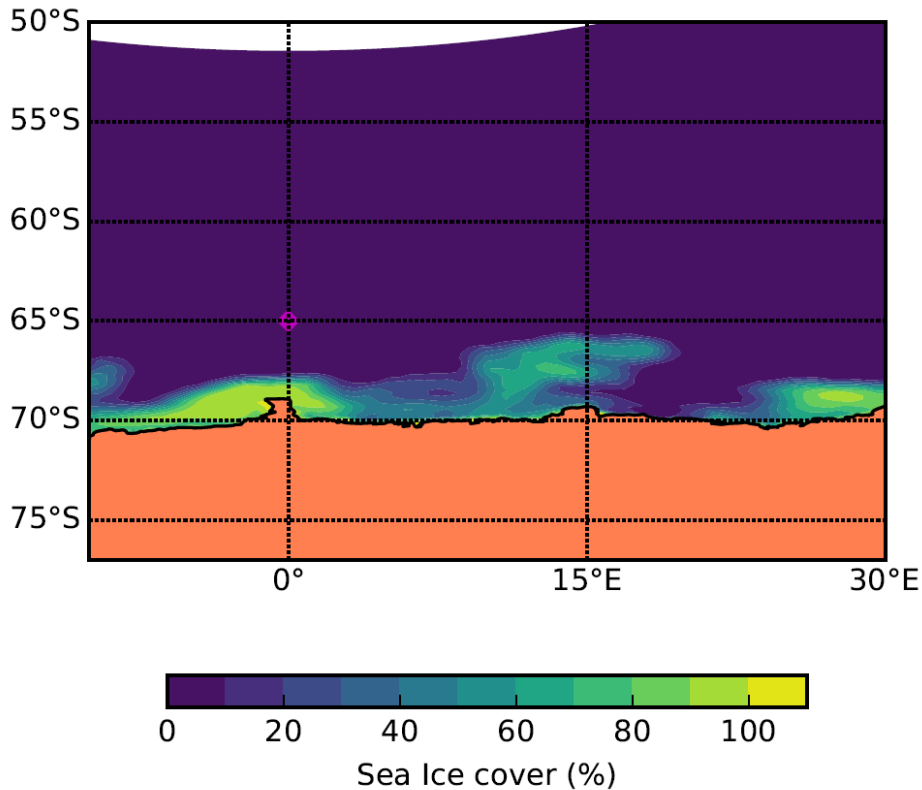


Figure S7. ODV contour plots of A) dissolved manganese (dMn, nmol/kg) and B) dissolved zinc (dZn, nmol/kg) on the GEOTRACES GIPY_05 cruise transect in the South Atlantic. Note the elevated concentrations in the surface and sub-surface hot spot around the Bouvet triple junction in the Antarctic Zone.

A)



B)

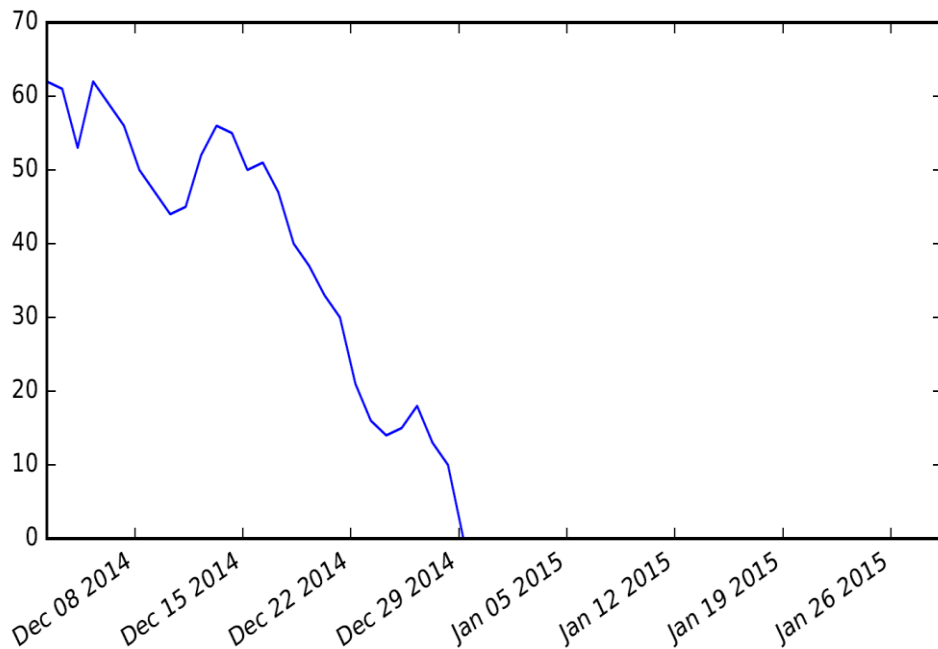


Figure S8. Panel A) sea-ice concentrations on 18 January 2015 (S54-65). Panel B) time-series of ice concentrations at the S54-65 site from December 2014 to January 2015 (SANAЕ54 cruise). Sea-ice concentrations were obtained from satellite imagery (Cavalieri et al. 1996, updated yearly).

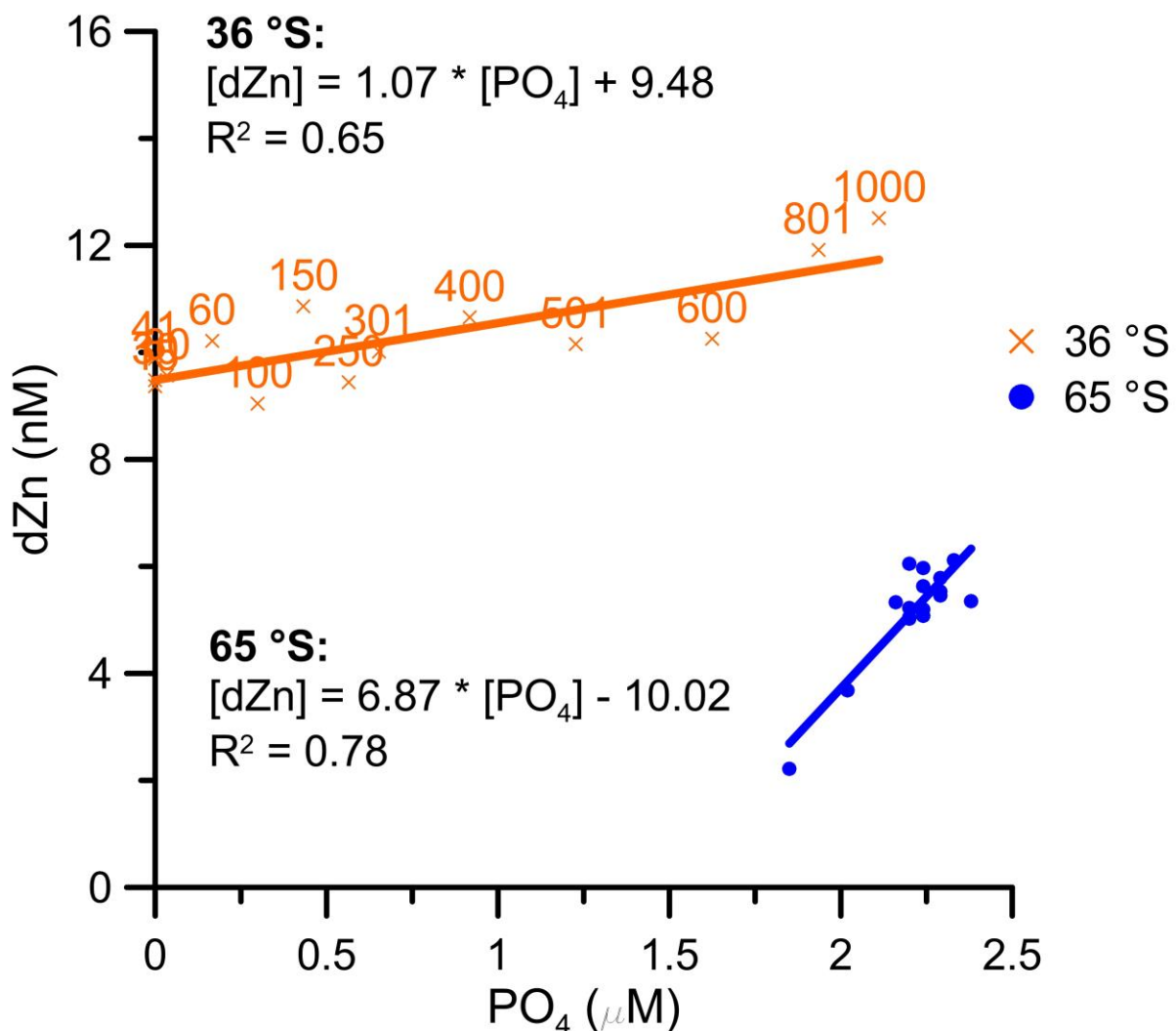


Figure S9. Metal:phosphate removal/uptake ratios explained: When the dissolved metal concentration over the vertical depth profile of a specific station is plotted against the corresponding dissolved phosphate (PO_4^{3-}) concentration profile, like in this figure, the resulting correlation trendline between the metal and phosphate can be used to infer the removal, or uptake if referred to biological removal, of that metal (Cloete et al. 2019 and references therein). Above, Zn is plotted against phosphate for the 36°S station, labels represent the water depth (m), of which produces a trendline with the equation: $[d\text{Zn}] = 1.07[\text{PO}_4] + 9.48$, that has a slope of 1.07 with the units nmol/ μmol (see main text table Table 3). This can be used to infer the removal/uptake of Zn in the water column: per 1 $\mu\text{mol/L}$ of phosphate removed, 1.07 nmol/L dissolved Zn is also removed. The steeper the slope of this correlation, as with the station at 65°S (slope = 6.87), the higher the uptake or use of the metal within the water column at a specific station.

4 References

- Arrigo, K. R. 1999. Phytoplankton Community Structure and the Drawdown of Nutrients and CO₂ in the Southern Ocean. *Science* (80-.). **283**: 365–367.
doi:10.1126/science.283.5400.365
- Baars, O., W. Abouchami, S. J. G. Galer, M. Boye, and P. L. Croot. 2014. Dissolved cadmium in the Southern Ocean: Distribution, speciation, and relation to phosphate. *Limnol. Oceanogr.* **59**: 385–399. doi:10.4319/lo.2014.59.2.0385
- Cavalieri, D. J., C. L. Parkinson, P. Gloersen, and H. J. Zwally. 1996. Sea ice concentrations from Nimbus-7 SMMR and DMSP SSM/I-SSMIS Passive Microwave Data, Version 1. [December 2013 - January 2015 daily data].doi:10.5067/8GQ8LZQL0VL
- Cloete, R., J. C. Loock, T. Mtshali, S. Fietz, and A. N. Roychoudhury. 2019. Winter and summer distributions of Copper, Zinc and Nickel along the International GEOTRACES Section GIPY05: Insights into deep winter mixing. *Chem. Geol.* **511**: 342–357.
doi:10.1016/J.CHEMGEOL.2018.10.023
- Croot, P. L., O. Baars, and P. Streu. 2011. The distribution of dissolved zinc in the Atlantic sector of the Southern Ocean. Deep Sea Res. Part II Top. Stud. Oceanogr. **58**: 2707–2719. doi:10.1016/J.DSR2.2010.10.041
- Cutter, G. A., and K. W. Bruland. 2012. Rapid and noncontaminating sampling system for trace elements in global ocean surveys. *Limnol. Oceanogr. Methods* **10**: 425–436.
doi:10.4319/lom.2012.10.425
- Cutter, G., L. Codispoti, P. Croot, R. Francois, M. Lohan, and M. Rutgers Van Der Loeff. 2014. Sampling and Sample-handling Protocols for GEOTRACES Cruises. **2**.
- DiTullio, G. R., N. Garcia, S. F. Riseman, and P. N. Sedwick. 2007. Effects of iron concentration on pigment composition in *Phaeocystis antarctica* grown at low irradiance. *Biogeochemistry* **83**: 71–81. doi:10.1007/978-1-4020-6214-8_7
- Gibberd, M. J., E. Kean, R. Barlow, S. Thomalla, and M. Lucas. 2013. Phytoplankton chemotaxonomy in the Atlantic sector of the Southern Ocean during late summer 2009. Deep. Res. Part I Oceanogr. Res. Pap. **78**: 70–78. doi:10.1016/j.dsr.2013.04.007
- Grasshoff, K., M. Ehrhardt, K. Kremling, and T. Almgren. 1983. Methods of seawater analysis, Verlag Chemie.
- Heller, M. I., and P. L. Croot. 2015. Copper speciation and distribution in the Atlantic sector of the Southern Ocean. *Mar. Chem.* **173**: 253–268. doi:10.1016/j.marchem.2014.09.017
- Kirchman, D. L., and P. A. Wheeler. 1998. Uptake of ammonium and nitrate by heterotrophic bacteria and phytoplankton in the sub-Arctic Pacific. Deep. Res. Part I Oceanogr. Res. Pap. **45**: 347–365. doi:10.1016/S0967-0637(97)00075-7
- Klunder, M. B., P. Laan, R. Middag, H. J. W. De Baar, and J. C. van Ooijen. 2011. Dissolved iron in the Southern Ocean (Atlantic sector). Deep. Res. Part II Top. Stud. Oceanogr. **58**: 2678–2694. doi:10.1016/j.dsr2.2010.10.042
- Löscher, B. M. 1999. Relationships among Ni, Cu, Zn, and major nutrients in the Southern Ocean. *Mar. Chem.* **67**: 67–102. doi:10.1016/S0304-4203(99)00050-X
- Mackey, M. D., D. J. Mackey, H. W. Higgins, and S. W. Wright. 1996. CHEMTAX- a program for estimating class abundances from chemical markers : application to HPLC measurements of phytoplankton. *Mar. Ecol. Prog. Ser.* **144**: 265–283.
doi:doi:10.3354/meps144265
- Mendes, C. R. B., R. Kerr, V. M. Tavano, F. A. Cavalheiro, C. A. E. Garcia, D. R. Gauns

- Dessai, and N. Anilkumar. 2015. Cross-front phytoplankton pigments and chemotaxonomic groups in the Indian sector of the Southern Ocean. Deep. Res. Part II Top. Stud. Oceanogr. **118**: 221–232. doi:10.1016/j.dsr2.2015.01.003
- Middag, R., H. J. W. de Baar, P. Laan, P. H. Cai, and J. C. van Ooijen. 2011. Dissolved manganese in the Atlantic sector of the Southern Ocean. Deep Sea Res. Part II Top. Stud. Oceanogr. **58**: 2661–2677. doi:10.1016/J.DSR2.2010.10.043
- NOAA. 2015. High density XBT transects: AX25.
- Orsi, A. H., T. Whitworth, and W. D. Nowlin. 1995. On the meridional extent and fronts of the Antarctic Circumpolar Current. Deep. Res. Part I **42**: 641–673. doi:10.1016/0967-0637(95)00021-W
- Pollard, R. T., M. I. Lucas, and J. F. Read. 2002. Physical controls on biogeochemical zonation in the Southern Ocean. Deep. Res. Part II Top. Stud. Oceanogr. **49**: 3289–3305. doi:10.1016/S0967-0645(02)00084-X
- Schlüter, L., P. Henriksen, T. G. Nielsen, and H. H. Jakobsen. 2011. Phytoplankton composition and biomass across the southern Indian Ocean. Deep Sea Res. Part I Oceanogr. Res. Pap. **58**: 546–556. doi:10.1016/j.dsr.2011.02.007
- Smith, W. O., and V. L. Asper. 2001. The influence of phytoplankton assemblage composition on biogeochemical characteristics and cycles in the southern Ross Sea, Antarctica. Deep. Res. Part I **48**: 137–161. doi:10.1016/S0967-0637(00)00045-5
- Viljoen, J. J., R. Philibert, N. Van Horsten, T. Mtshali, A. N. Roychoudhury, S. Thomalla, and S. Fietz. 2018. Phytoplankton response in growth, photophysiology and community structure to iron and light in the Polar Frontal Zone and Antarctic waters. Deep. Res. Part I Oceanogr. Res. Pap. **141**: 118–129. doi:10.1016/j.dsr.2018.09.006
- Wright, S. W., R. L. van den Enden, I. Pearce, A. T. Davidson, F. J. Scott, and K. J. Westwood. 2010. Phytoplankton community structure and stocks in the Southern Ocean (30–80°E) determined by CHEMTAX analysis of HPLC pigment signatures. Deep. Res. Part II Top. Stud. Oceanogr. **57**: 758–778. doi:10.1016/j.dsr2.2009.06.015